

Exploring the dissipative regime of superconductors for practical current-lead applications

Milind N. Kunchur,^{a)} D. K. Christen, and C. E. Klabunde

Solid State Division, Oak Ridge National Laboratory, P. O. Box 2008, Oak Ridge, Tennessee 37831-6057

Kamel Salama

Texas Center for Superconductivity and Mechanical Engineering Department, University of Houston, Houston, Texas 77204-4792

(Received 3 March 1995; accepted for publication 29 May 1995)

A pulsed-current technique was used to measure the extended I - V characteristics of a wide variety of prototype high-temperature-superconductor (HTS) leads. It was found that the average resistivity rises with $J(>J_c)$ more gradually than in conventional superconductors—often remaining very small compared to silver, for values of $J(\gg J_c)$ that are high enough to be practically useful. This observation, combined with the low thermal conductivity (~ 50 times smaller than Ag), should extend the utility of HTS leads to the dissipative regime where $J/J_c \gg 1$. © 1995 American Institute of Physics.

Perfect electrical conduction is a hallmark property of superconductivity. For conventional superconductors in the form of thin wires, the critical current density J_c , which signals onset of resistance, can indeed be comparable to the depairing current density J_d , which demarcates the mean-field phase boundary where the order parameter Δ vanishes. In general, however, vanishing resistance is not a defining property of the superconducting state. In high-temperature superconductors (HTSs) there is often a wide dissipative regime^{1,2} between J_c and J_d . While J_d is sufficiently high ($\sim 10^9$ A/cm² at $T=0$), J_c tends to be disappointingly low because of flux motion and various extrinsic effects, and has been viewed as a significant obstacle for practical applications of HTS materials.

In this letter we consider a different approach for judging the practical utility of HTS materials. The very property that weakens J_c through flux motion (reduced pinning strength because of small ξ , i.e., large H_{c2}) can allow the resistivity to remain very small ($\rho < \rho_n \times B/H_{c2}$) for $J \gg J_c$. With the exception of a persistent-mode superconductive magnet, few applications require absolutely perfect conduction. In particular current leads connecting to a cryogenic device (e.g., superconductive magnet), or a power transmission line, merely require a resistivity that is as low as possible compared to alternative normal-metal conductors (such as silver or copper) at a given temperature. A HTS lead with a small average relative resistivity ($\rho_{\text{rel}} = \rho_{\text{HTS}}/\rho_{\text{Ag}}$) at the required J would therefore be useful for such applications. In addition to a possible low ρ_{rel} , high-temperature superconductors intrinsically have low thermal conductivity, which can reduce heat conduction into a cryogenic system.

In this work we investigate the behavior of several prototype HTS conductors up to current densities well above J_c to study ρ_{rel} as a function of J . In order to reduce heating at contacts, a pulsed-current method was used for the measurements. (Because the segments tested were short, good contacts could not be made easily. In an actual application,

contacts can be made over longer portions of the conductor.) The studies were conducted at $T=77$ K and zero applied magnetic field (i.e., self-field of the current), since the goal was to explore the performance in current-lead applications. In most cases $\rho_{\text{rel}}(J)$ rises gradually with J/J_c , and remains small at usefully high current densities even for specimens with low J_c .

The calculation of $\rho_{\text{rel}}(J)$ is an extremely complex task—influenced by numerous intrinsic and extrinsic mechanisms; so a comprehensive theoretical treatment of the dissipation will not be attempted here. However, some qualitative statements can be made. First of all at the temperature ($T=77$ K) and currents ($J < 10^6$ A/cm² $\ll J_d$) of interest, the dissipation arising from phase slippage and thermal fluctuations is negligible.³⁻⁵ The dominant causes of dissipation will be (1) the motion of flux vortices associated with the self-field of the transport current and (2) resistance across grain boundaries (GBs) and other types of weak links. In addition once the superconductor itself becomes dissipative, current will flow through coexisting normal paths, which may be present because of sample inhomogeneity or by design (e.g., a superconductor sheathed in silver). At any given point in the specimen the dissipation arising from flux motion ρ_{fm} is a function of the local values of B and J , and the flux pinning strength. As was shown in earlier work,^{1,6} at typical current densities pinning causes ρ_{fm} to be greatly suppressed below the free-flux-flow resistivity: $\rho_{\text{fm}} \ll \rho_{\text{fff}} \approx \rho_n \times B_{\text{self}}/H_{c2}$. The experimentally measured average quantity $\rho_{\text{rel}}(J)$, will be governed not only by the local $\rho(B, J)$ characteristic of the material, but also by the size and shape of the specimen. For a given J , a cross section that is larger in its area or aspect ratio will have a B field that is less spatially uniform, with higher values at the edges. This will lead to a reduced J_c and more gradual $\rho_{\text{rel}}(J)$. Sample inhomogeneity can affect $\rho_{\text{rel}}(J)$ in several ways. Fine-scale disorder can aid pinning, increasing J_c and making $\rho_{\text{rel}}(J)$ steeper. Large-scale inhomogeneity on the other hand will result in regions that are normal or weakly superconducting that essentially exclude current, forcing it to flow along tor-

^{a)}Electronic mail: m6v@solid.ssd.ornl.gov

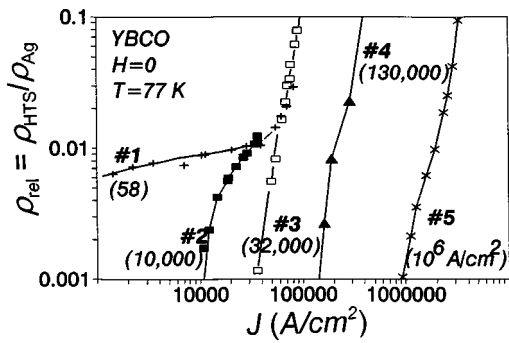


FIG. 1. Relative resistivity vs J for five YBCO samples; $\rho_{Ag}=0.28 \mu\Omega \text{ cm}$. Quantities in parentheses are J_c 's at $E \sim 1 \mu\text{V/cm}$. Melt-textured samples 1, 2, and 3 (with weak, strong, and no grain boundaries, respectively) show convergence in $\rho_{rel}(J)$ for $J \gg J_c$.

tuous percolative paths of strongly linked material. The behavior of the strongly coupled paths in samples made by different processes might have similar characteristics. An interesting situation arises when a defect, such as a GB, traverses the entire sample cross section. The observed J_c and ρ_{rel} just above J_c will be governed entirely by the response of the GB. In particular if the GB is weakly coupled, there will be a precipitous drop in J_c . However, when $J \gg J_c$, and the superconductor is intrinsically dissipative, the resistance across the GB can become a small fractional contribution. As a result at high J 's the $\rho_{rel}(J)$ function may be insensitive to such defects. The data presented and analyzed in the remainder of this letter explore and support these qualitative ideas.

Eight samples were included in this study: samples No. 1, 2, and 3 are melt-textured rods of $Y_1\text{Ba}_2\text{Cu}_3\text{O}_{7-\delta}$ (YBCO) with cross sections 1.6×1.6 , 0.6×0.6 , and $0.3 \times 0.4 \text{ mm}^2$, respectively; No. 4 is a zone melt-processed YBCO filament of $190 \mu\text{m}$ diameter; No. 5 is a 100 nm thick, $100 \mu\text{m}$ wide YBCO epitaxial film on LaAlO_3 ; No. 6 and No. 7 are oxide-powder-in-tube (OPIT) tapes of $\text{Bi}_2\text{Sr}_2\text{Ca}_2\text{Cu}_3\text{O}_8$ (BSCCO) in a silver matrix with multifilamentary and monocoil structures, respectively, and outside cross sections of 0.173×5.3 and $0.15 \times 5.0 \text{ mm}^2$ (of which the BSCCO comprises 20%–25% by area); No. 8 is an unpatterned $3 \mu\text{m}$ thick, 5.1 mm wide $\text{TlBa}_2\text{Ca}_2\text{Cu}_3\text{O}_x$ (TBCCO) film deposited on $250 \mu\text{m}$ thick polycrystalline silver.

Distances between voltage leads were a few mm; the samples themselves are longer. Contacts were made with either silver paint or sputtered gold followed by annealing at 550°C . All contact resistances were under $100 \mu\Omega$.

The I - V data were measured using a four-probe pulsed-current technique to reduce heating from internal dissipation and at contacts. The functional description of the technique and associated calibration procedures and tests are published elsewhere.¹ $\rho_{rel} = \rho_{HTS}/\rho_{Ag}$ is calculated using $\rho_{Ag} = 0.28 \mu\Omega \text{ cm}$ at 77 K .⁷

Figure 1 shows ρ_{rel} vs J for the five YBCO samples. Sample Nos. 1, 2, and 3 illustrate the dramatic change in J_c caused by the presence of grain boundaries that traverse the entire cross section. Going from no GB (No. 3) to a weakly coupled GB (No. 1), one finds J_c to change by three orders of magnitude. Nevertheless at higher dissipation

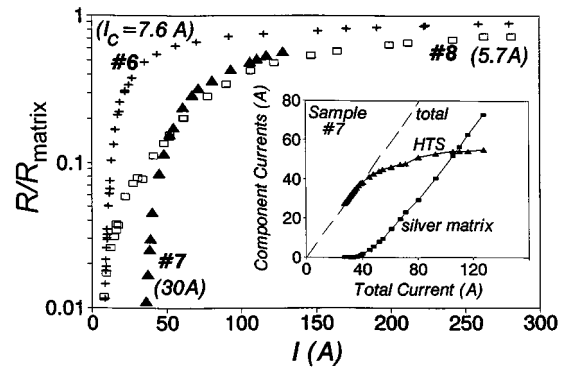


FIG. 2. HTS/Ag composite conductors. R_{matrix} is the resistance of the silver encapsulation. I_c 's (at $E \sim 1 \mu\text{V/cm}$) are shown in parentheses. Inset shows how the total current partitions between the superconductor (HTS) and silver.

levels—where the fractional resistance across the GBs becomes irrelevant—the curves overlap as anticipated earlier. Thus a resistively defined “ J_c ” at say $\rho_{rel} = 2\%$ of silver is not only much higher ($\sim 6 \times 10^4 \text{ A/cm}^2$) than the usual J_c (at $E \sim 1 \mu\text{V/cm}$), but less dependent on sample defects and therefore more reproducible. The $\rho_{rel}(J)$'s for the other two YBCO samples (Nos. 4 and 5) are discussed later.

Figure 2 depicts the three HTS/Ag composite conductors. For these there are two separate types of characteristics that are of interest: (1) the observed resistance of the overall conductor as a function of the total current, and (2) the intrinsic response of the superconductive component. The first type of characteristic is plotted in Fig. 2. The ordinate is not the previous ρ_{rel} , but is the observed R scaled by R_{Ag} of the silver matrix—the limiting resistance when the superconductor is driven normal (since $\rho_n \gg \rho_{Ag}$). In the BSCCO/Ag tapes (Nos. 6 and 7), the current is driven into the silver matrix rather quickly above I_c . For the TBCCO/Ag tape (No. 8), remarkably, the overall resistance remains suppressed well below R_{Ag} for currents ten times I_c , even though the HTS component comprises only 1% of the cross section. The inset shows how the total current partitions between the superconductor and matrix for one of the samples (No. 7). The bottom curve in the inset (I_{matrix} vs I_{total}) is proportional to the overall I - V characteristic since $V = R_{matrix} \times I_{matrix}$. The observation of a linear I - V with an intercept is of fundamental and historical significance. Such a precursor linear region of the I - V characteristic may have been mistaken for flux flow in earlier work.⁸ In Fig. 2 (inset) the slope reflects the R of the silver and is unrelated to flux flow.⁹

The final graph (Fig. 3) compares $\rho_{rel}(J/J_c)$ for the strongly coupled samples (Nos. 1 and 2 with transverse GBs are excluded.) For the composite conductors (Nos. 6, 7, and 8), the intrinsic characteristics were extracted from the measured behavior using a parallel-conductor model. As expected the film samples (Nos. 5 and 8)—with their strongly demagnetizing geometries—have the most gradual $\rho_{rel}(J/J_c)$ functions. The TBCCO has a lower J_c (weaker flux pinning) but a higher H_{c2} and J_d because its $T/T_c \approx 0.7$ instead of 0.9 for YBCO. Accordingly it has the most gradual $\rho_{rel}(J/J_c)$, its resistivity remaining three orders

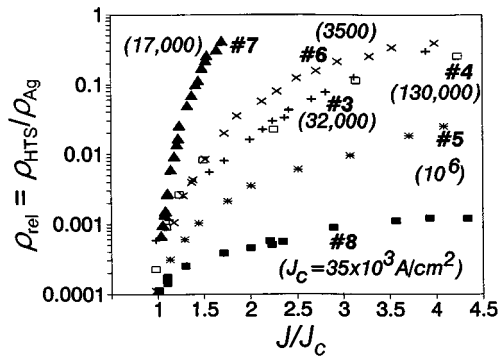


FIG. 3. Relative resistivity of the superconducting component as a function J/J_c . The J_c 's (at $E \sim 1 \mu\text{V/cm}$) are indicated in parentheses.

of magnitude below silver even at five times the critical current. Sample Nos. 3 and 4 have the same material, and similar cross-sectional size and shape. Accordingly their $\rho_{rel}(J/J_c)$ functions are roughly the same. Between the two BSCCO/Ag conductors, the one with the higher J_c has a steeper $\rho_{rel}(J/J_c)$ function as expected, since their J_d 's ought to be comparable. For all samples the measured ρ is always much lower than $\rho_{\text{eff}} \approx \rho_n \times B_{\text{self}}/H_{c2}$ calculated from the estimated self-field, showing that pinning drastically suppresses the dissipation for these J values.^{1,6}

To summarize, the $\rho_{rel}(J)$ characteristics of several practical HTS conductors were measured well above J_c . In all cases ρ remains below that of silver up to $J \sim 2J_c$ and in some cases two to three orders of magnitude below silver at several times J_c . These data demonstrate the potential use of HTS conductors at currents considerably above the critical value, while maintaining a very low power dissipation rate. As an example, the "pencil-lead" (0.6 mm square) shaped sample No. 2, can maintain $\rho_{rel} < 1\%$, while carrying $I = 100 \text{ A}$ ($J = 28\,000 \text{ A/cm}^2$); this corresponds to an internal dissipation of only 0.8 W/m and a liquid-nitrogen-boil-off rate of 18 ml/h. Because the present data were measured with pulsed currents, the additional problem of thermal stability

for continuous currents must be considered separately to evaluate feasibility of a steady-state application. The $\rho_{rel}(J)$ information provided here should, however, be directly relevant for applications that involve low-duty-cycle signals with large transient peaks, such as the music signal between an audio amplifier and a speaker.

The authors wish to acknowledge the following for supplying materials used in this work: Straightwire, Ceramic Processing Systems-Superconductivity, American Superconductor Corp., AT&T Bell Laboratories, Intermagnetics General Corp., the Metals and Ceramics Division at Oak Ridge National Laboratory, and H. R. Kerchner for discussions. Research cosponsored by the DOE Division of Materials Sciences, and by the DOE Office of Advanced Utility Concepts, Superconductivity Program for Electric Power Systems, both under Contract No. DE-AC05-84OR21400 with Martin Marietta Systems, Inc. Partial support for the program was administered by the Oak Ridge Institute for Science and Education, and additional partial support was made by the State of Texas.

- ¹M. N. Kunchur, *Mod. Phys. Lett. B* **9**, 399 (1995).
- ²M. N. Kunchur, D. K. Christen, C. E. Klabunde, and J. M. Phillips, *Phys. Rev. Lett.* **72**, 752 (1994).
- ³Michael Tinkham, *Introduction to Superconductivity* (McGraw Hill, New York, 1975).
- ⁴V. Ambegaokar, in *Superconductivity*, edited by P. R. Wallace (Gordon and Breach, New York, 1969), Ch. 2, Vol. 1, and references therein.
- ⁵B. I. Ivlev and N. B. Kopnin, *Adv. Phys.* **33**, 47 (1984), and references therein.
- ⁶M. N. Kunchur, D. K. Christen, and J. M. Phillips, *Phys. Rev. Lett.* **70**, 998 (1993).
- ⁷R. A. Matula, *J. Phys. Chem. Ref. Data* **8**, 1147 (1979); D. R. Smith and F. R. Fickett, *Cryogenic Properties of Silver*, Chart no. 1994-574-385 from the National Institute of Standards and Technology (Superintendent of Documents, U.S. Government printing office, Washington, 1994).
- ⁸Y. B. Kim, C. F. Hempstead, and A. R. Strnad, *Phys. Rev. A* **139**, 1163 (1965).
- ⁹It should be noted, however, that a linear I - V curve with finite intercept and approximate free-flux-flow slope has been theoretically predicted for certain specialized types of flux motion, e.g., see G. Blatter, M. V. Feigel'man, V. B. Geshkenbein, A. I. Larkin, and V. M. Vinokur, *Rev. Mod. Phys.* **66**, 1125 (1994).